Production of fuel-cell grade hydrogen by sorption enhanced water gas shift reaction using Pd/Ni-Co catalyst

Tayyaba Noor[a], María V. Gil[b], De Chen[a],*

[a] *Department of Chemical Engineering, Norwegian University of Science and Technology, Sem Sælands vei 4, Trondheim, NO-7491, Norway*

[b] *Instituto Nacional del Carbón, INCAR-CSIC, Apartado 73, 33080 Oviedo, Spain*

Abstract

It has been demonstrated both thermodynamically and experimentally that fuel-cell grade hydrogen can be produced by a one-step sorption enhanced water gas shift (SEWGS) process at about 500 ℃, where the water gas shift (WGS) catalyst and the CO_2 sorbent are highly integrated. A synthetic CaO-based mixed oxide sorbent was also assessed, which showed a good CO_2 capture capacity and stability in the cyclic operation of the SEWGS reaction. Catalysts play a significant role in CO conversion via WGS, methanation and methane steam reforming reactions. A Pd promoted Ni-Co catalyst (1%Pd/20%Ni-20%Co) derived from hydrotalcite-like material (HT) showed a high activity for WGS and methane steam reforming. The methanation activity was further reduced on 30%Ni-10%Co. There exists an optimum temperature (500 ℃) for hydrogen production by the SEWGS process, where it is kinetically limited by the WGS reaction at low temperatures (425-475 ℃) and it is thermodynamically unfavorable at higher temperatures (475-550 ℃). The challenges for hydrogen production by SEWGS at high CO pressures were also demonstrated, where CO pressure has shown a negative

* Corresponding author. Tel.: +47 73593149; fax: +47 73595047.

E-mail address: chen@nt.ntnu.no (D. Chen).

influence on WGS activity. An induction period was observed, which can be reduced by improving catalyst activity and by adding hydrogen to the reactant mixture.

1. Introduction

Hydrogen is an environmentally friendly and clean energy carrier for a sustainable energy system. In the last few decades, much research has been focused on the study of the benefits and challenges of establishing a cost-effective hydrogen economy. Currently, global hydrogen production comes from natural gas (48%), oil (30%) and coal (18%), water electrolysis accounting for only 4% [1]. Hydrogen has been widely used for the production of ammonia fertilizers via the Haber process, for methanol synthesis and for conversion of heavy petroleum sources to lighter fractions via hydrocracking [2]. The worldwide demand for hydrogen is expected to increase in the future, not only for conventional industrial uses, but also for clean energy generation such as by means of fuel cells. The development of less expensive methods of producing pure hydrogen is needed to achieve a hydrogen economy.

Literature studies show that by the year 2030, about 10% of the worldwide yearly energy consumption will be derived from the water gas shift (WGS) reaction [3,4]. The WGS reaction is extensively used to increase the H_2 content in the synthesis gas containing CO, H_2, CO_2 and H_2O, which can be generated from the reforming of hydrocarbons from fossil fuels, coal and biomass [5]. To eliminate CO from the synthesis gas, the WGS reaction plays a vital role in further downstream industrial

practices, e.g. production of hydrogen, ammonia, methanol and several other chemicals [6]. The CO reacts with H_2O to produce CO_2 and H_2 through the reaction shown in Equation (1):

$$CO_{(g)} + H_2O_{(g)} \leftrightarrow H_{2(g)} + CO_{2(g)} \qquad \Delta H^0 = -41.2 \text{ kJ mol}^{-1} \qquad (1)$$
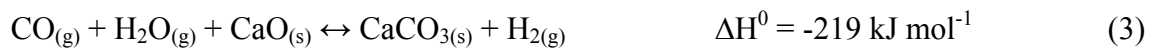
It is a reversible and moderately exothermic reaction. Lower temperature thermodynamically favors the CO conversion. For reaching a high process effectiveness, the shift reaction is industrially performed in two stages, i.e., high temperature shift (300-500 ºC) followed by a low temperature shift (180-250 ºC). The high temperature reactor converts bulk CO from ~15% to ~3% and the low temperature unit further reduces the CO level to less than 0.4% [7,8]. However, in order to produce high-purity H_2, additional purification processes are required, such as the pressure swing adsorption (PSA) process. More than 22% of the cost of producing a purified hydrogen stream comes from the CO_2 separation process carried out to increase the hydrogen purity in the exhaust gas, as additional energy and equipment are required [9]. The WGS reaction has also acquired major importance in fuel processing as a CO removal method in hydrogen production for fuel cells. Low temperature proton exchange membrane (PEM) fuel cells [10] require very low CO levels (<10 ppm) in the H_2-rich gas stream in order to suppress the poisoning effect of CO to the PEM fuel cell catalysts. Production of highly pure hydrogen is of paramount importance for overcoming the CO poisoning problem. In addition to the WGS reaction, a preferential oxidation (PrOx) step is usually implemented in fuel processing, in which most of the residual CO is oxidized to CO_2. However, a more energy effective technology for production of highly pure hydrogen is extremely desired for using in PEM fuel cells.

Hydrogen production by "sorption enhanced" processes is one of the most promising approaches for one-step production of high-purity hydrogen which could greatly simplify the process, increase the energy efficiency and lower the cost, as reviewed by Harrison [11], Barelli et al. [12], as well as Chen and He [13]. The sorption enhanced concept is based on the Le Chatelier's principle, i.e., in an equilibrium-limited reaction, the shift of the forward reaction to the product side can be enhanced by selective removal of a reaction product from the reaction mixture. With the aim of avoiding a further purification step in hydrogen production, this concept has been applied to the WGS reaction by several researchers [14,15] by employing a CO_2 sorbent which captures the CO_2 from the gas phase achieving enhanced yield and conversion values, so that a stream of pure H_2 can be produced.

In the sorption enhanced water gas shift (SEWGS) process, a mixture of a CO_2 sorbent and a WGS catalyst is installed in a single unit. SEWGS can be divided into two categories, mediate-temperature one (250-350 ºC) on modified hydrotalcites, and high-temperature one on CaO and other mixed oxides sorbents (400-650 ºC). The operating temperature depends mostly on thermodynamic properties of the CO_2 acceptors. For mediate-temperature SEWGS reaction, hydrotalcites are the commonly chosen sorbents, although their CO_2 adsorption capacity is relatively low (1-2 wt%) and adsorption/desorption kinetics is poor at the reaction and regeneration conditions. Enhanced hydrogen production along with almost 100% CO conversion has been illustrated by the SEWGS process at 400 ºC on potassium-promoted hydrotalcite-based materials as CO_2 acceptors and commercially available iron-chromium-based shift catalysts [16,17]. Jang et al. [18] recently reported the use of K_2CO_3-promoted hydrotalcite and Na_2O-promoted alumina as CO_2 sorbents along with a commercial low

temperature shift catalyst in the SEWGS process at 400 ℃ to generate high-purity hydrogen. Fuel-cell grade hydrogen (<10-20 ppm CO) has been also obtained by Beaver et al. [19] from the SEWGS process at reaction temperatures of 200 ℃ using K_2CO_3-promoted hydrotalcite and Na_2O-promoted alumina sorbents and a commercial WGS catalyst. Hydrotalcites with alkaline metal oxides promotion enhanced the CO_2 capture. However, alkaline metals such as Na and K are mobile in steam, so they have been reported as poisons which deactivate the steam reforming catalysts [20]. However, such effects have not been addressed in the SEWGS with alkaline promoted hydrotalcites and cycle stability of SEWGS using alkaline oxides promoted hydrotalcites has not been reported.

On the other hand, CaO-based sorbents are typically a common choice for CO_2 capture purposes along with commercial catalysts at high temperatures [15]. The major advantages of CaO-based materials are that they exhibit fairly good kinetics and excellent adsorption capacity at high temperatures (20-50 wt%), together with that their raw materials (i.e., limestone or dolomite) are abundant and inexpensive. The sorption reaction using CaO as sorbent material is represented by Equation (2), whereas the overall SEWGS is expressed as shown in Equation (3):

$$CaO_{(s)} + CO_{2(g)} \leftrightarrow CaCO_{3(s)} \qquad\qquad \Delta H^0 = \text{-178 kJ mol}^{-1} \qquad (2)$$

$$CO_{(g)} + H_2O_{(g)} + CaO_{(s)} \leftrightarrow CaCO_{3(s)} + H_{2(g)} \qquad \Delta H^0 = \text{-219 kJ mol}^{-1} \qquad (3)$$

The earliest concept of the SEWGS process using CaO-based sorbents (dolomite), traces back in 1931, when Gluud et al. [21] proposed to carry out the SEWGS reaction at temperatures of 300-600 ℃, assuming that CaO plays an active role in the CO_2 capture shifting the reaction towards forward direction. Han and Harrison [22] in 1994 confirmed the enhancement of the reaction efficiency at 500-600 ℃ using dolomite as

CO_2 sorbent without any catalyst in SEWGS experiments. The high-temperature SEWGS is superior to the mediate-temperature SEWGS regarding to the process energy efficiency, due to a smaller gap of the temperature in relation to the synthesis gas production [23]. In addition, higher rates for both WGS and carbonation reactions as well as high CO_2 capture capacity of CaO-based materials could significantly reduce the reactor value required.

Ramkumar and Fan [24] also demonstrated the enhanced hydrogen yield from coal-derived syngas using a synthetic CaO sorbent and a commercial high-temperature WGS catalyst and they obtained a hydrogen purity >99% at high pressures. The presence of WGS catalyst clearly improved the hydrogen production, particularly at low pressures. Unfortunately their reactor system had a relatively large contribution to WGS reaction, making it difficult to analyze the effects of catalyst in SEWGS. In addition, cyclic stability of the sorbents has not been reported. Müller et al. [14] compared natural and synthetic CaO-based sorbents in SEWGS experiments at 650 ºC, revealing a constant decline in the hydrogen production over a number of cycles using limestone. Synthetic calcium magnesium acetate was found to be more stable than the natural CaO-based sorbents. The key drawback of CaO-based sorbents is that the chemically reactive CaO is a weak, friable material with poor cycle stability. Calcined dolomite (CaO/MgO) has been proved to be a good natural material for CO_2 capture [13,25,26] which has better multi-cycle properties compared to limestone [27,28]. However, dolomites suffer serious deactivation during cycles. The improvement in the properties of CaO-based sorbents for being used in SEWGS processes still represents an important challenge. Large efforts have been devoted to develop new synthetic CO_2 solid sorbents for high-temperature sorption enhanced processes, such as lithium silicates and zirconates [29],

sodium zirconate [30,31] and synthetic CaO-based solid sorbents [32,33]. These synthetic CO_2 acceptors were found to significantly improve the cyclic behavior at high temperatures, so they have become highly attractive for being used in SEWGS processes.

Apart from the sorbent material, highly active catalysts are also crucial for obtaining high yield and high purity of hydrogen, in particular fuel-cell grade hydrogen, from sorption enhanced reactions. Few literature reports are available on the study of catalysts under SEWGS conditions and most likely industrial catalysts are employed. The performance of Fe-Cr and Co-Mo as promising catalysts under SEWGS conditions at 400 ºC was illustrated by van Dijk et al. [34]. The typically used industrial catalyst for the high-temperature WGS reaction is usually a combination of Fe_2O_3 and Cr_2O_3 [35], but due to the toxic and carcinogenic issues of chromium, it is highly desirable to develop an alternative chromium-free catalyst for being used in this process. Some chromium-free iron-based catalysts containing Al, Ni, Co and Zn have been studied with satisfactory results [36,37]. The effectiveness in the CO conversion on different metals supported on alumina at high temperatures (300-1000 ºC) has been found to follow the following order: Ni>Ru>Rh>Pt>Pd [38]. The commercial $Cu/ZnO/Al_2O_3$ catalyst is widely used in industrial fields for the low-temperature WGS reaction, but other materials like ceria-supported transition metals catalysts have been studied showing high activities for the WGS reaction [39].

Nickel-based catalysts have been also studied for both high- and low-temperature WGS reaction. Addition of K as promoter in Ni-based catalysts improved the activity and selectivity for the WGS reaction [40]. Ni-based catalysts were also studied on different supports like SiO_2 and Al_2O_3 [41]. Previous works in our research group showed high

activity and stability for the H_2 production from biomass reforming using a bimetallic Ni-Co catalyst [42-44]. A Ni-Co catalyst derived from hydrotalcite-like material (HT) was also synthesized and studied in sorption enhanced steam reforming (SESR) of ethanol [45] and glycerol [46]. A previous effort carried out by our research group concerning sorption enhanced studies of the WGS reaction was based on biosyngas [47] using a 30%Ni-10%Co HT catalyst, showing that the process was highly proficient to produce relatively pure H_2, but the CO content was still too high for direct use in PEM fuel cells.

The present work is focused on the development of new catalyst and sorbent materials appropriate for using in the high-temperature SEWGS reaction aiming for one-step production of fuel-cell grade high-purity hydrogen (<10 ppm CO) with low concentrations of CO_2 and methane, which has not been previously reported in literature. 1%Pd/20%Ni-20%Co, 20%Ni-20%Co and 30%Ni-10%Co HT-derived catalysts were used to study the effect of the catalyst composition (Co/Ni ratios) and that of the addition of Pd in the catalyst on the SEWGS reaction, aiming for high WGS activity and low methanation activity. Calcined dolomite and a synthetic nano-crystalline mixed oxide (CaCeZr) were studied as CO_2 sorbent materials in the SEWGS process in order to achieve a better sorbent stability. The operating temperature, steam/CO ratio and CO partial pressure in the feed stream were thermodynamically and experimentally assessed in order to obtain pure H_2 in the one-step proposed process. An additional objective of the present work is to gain a better understanding of the SEWGS reaction, which integrates sorption enhanced and reforming reactions.

2. Experimental

Several Ni-Co hydrotalcite-like materials (HT) have been used as catalysts in this work: 20%Ni-20%Co HT, 30%Ni-10%Co HT and 1%Pd/20%Ni-20%Co HT. The Ni-Co HT catalysts were prepared by co-precipitation of $Ni(NO_3)_2 \cdot 6H_2O$, $Co(NO_3)_3 \cdot 6H_2O$, $Mg(NO_3)_3 \cdot 6H_2O$ and $Al(NO_3)_3 \cdot 9H_2O$. The stoichiometric ratio of cations was chosen to yield 40 wt% total metal loading of Ni and Co, giving materials with the nominal compositions of 20%Ni-20%Co and 30%Ni-10%Co. The collected precipitates were washed, dried and calcined at 600 ºC for 6 h to yield the Ni-Co HT. A detailed description of the Ni-Co HT catalyst preparation and characterization was reported elsewhere [43,48]. The 20%Ni-20%Co HT catalyst was used as precursor of the Ni-Co HT catalyst promoted with Pd, 1%Pd/20%Ni-20%Co HT, which was prepared by the incipient wetness method. After calcination, the 20%Ni-20%Co HT was impregnated with a 1% (w/w) loading of Pd. The Pd solution was prepared by dissolving $PdCl_2$ into two equivalents of HCl and diluting in ethanol to the desired concentration. The sample was then dried for 14 h at 100 ºC and calcined at 500 ºC for 1 h. Finally, the calcined catalysts were pelletized, ground and sieved to the desired particle size (250-500 μm).

Two CO_2 sorbents were used in the SEWGS experiments in the present work: calcined dolomite and a CaO-based mixed oxide (CaCeZr). ARCTIC dolomite, precursor of the CO_2 acceptor, was supplied by Franefoss Miljøkalk As, Norway. It had a purity of approximately 98.5 wt% $CaMg(CO_3)_2$ and no sulfur according to X-ray fluorescence analysis. The dolomite sample was calcined in an air flow at 750 ºC for 4 h prior to its application as CO_2 sorbent. Its initial maximum capacity for CO_2 capture was estimated at ca. 46% (weight of captured CO_2/weight of sorbent). The second sorbent was a calcium-based mixed oxide developed to study its stability and performance in the

SEWGS process. The mixed oxide CaCeZr was prepared by using the spray drying technique [49]. The precursor slurry was prepared by mixing the metal salts, calcium acetate (Fluka), cerium nitrate (Fluka) and zirconium nitrate (Fluka), at a molar ratio of 10:1:1 in deionized water. The solution was stirred overnight and the slurry was subjected to spray drying (Buchi, Mini Spray drier, B-191) at 200 ºC. The pump speed was adjusted to reach a solution intake of 8 mL min^{-1} and the air flow was 4.3 m s^{-1}. The product obtained after spray drying was calcined at 750 ºC for 4 h under air flow and it was ready to be used as sorbent material.

XRD and nitrogen physisorption analyses were carried out in order to characterize catalyst and sorbent materials. The crystalline structure of the materials was studied by powder X-ray diffraction analysis on a Siemens IFFRACplus-D5005 diffractometer. Nitrogen physisorption measurements were performed on a Micromeritics Tristar 3000 at -196 ºC after outgassing the samples overnight under vacuum at 100 ºC before adsorption. The surface area was calculated using the BET equation in the relative pressure interval ranging from 0.01 to 0.30. The adsorption average pore width (4 V/A) was estimated by the Barret-Joyner-Halenda (BJH) method provided by the Micromeritics Tristar 3000 built-in software.

The SEWGS experiments were carried out in a Microactivity-Reference reactor (PID Eng&Tech, Spain). The schematic diagram of the experimental setup is shown in Fig. 1. A mixture of catalyst and sorbent was place in a fixed bed quartz reactor (inner diameter 14 mm). Prior to the experiment, the catalyst was activated by reduction at 670 ºC for 10 h under a flowing gas mixture of 50 vol% H_2-He (total flow 200 mL min^{-1}) and the reactor was then purged with inert gas and cooled down to the desired temperature. The reaction temperature was monitored by means of a thermocouple inserted in the bed. All

the experiments were carried out at atmospheric pressure in the temperature range of 425 ºC-550 ºC to study the effect of the reaction temperature. The steam/CO ratio and the CO partial pressure in the feed stream were varied in the different experiments in order to evaluate their effect on the SEWGS reaction. For the SEWGS experiments, a vapor mixture of CO and H_2O was swept by He flow into the reactor. Gases were delivered by Bronkhorst mass flow controllers and liquid water was introduced by a Gilson® HPLC pump and vaporized by means of an evaporator before being introduced into the reactor. The reactor effluent was cooled down through a condenser (Peltier) and an ice-cooled bath. The exiting gas was analyzed with an online Agilent 3000 Micro GC equipped with a Molsieve and a Plot U columns and a TCD detector. The Micro GC was calibrated employing a standard gas mixture at periodical intervals and the detection limit of the equipment is 0.001 vol%. The SEWGS reaction occurred until the CO_2 sorbent was saturated and it lost the capacity for CO_2 removal. For the study of the sorbent stability, after the SEWGS experiment the feed was switched to inert gas for sorbent regeneration at 750 ºC for about 4 h and the reaction and regeneration stages were repeated cyclically.

The product gas distribution was based on the water-free composition of the gas effluent. The results were expressed as molar fraction of H_2, CO, CH_4 and CO_2. The capture capacity of the CaCeZr mixed-oxide sorbent in the cyclic operation was calculated by Equation (4) and it was expressed as grams of CO_2 captured per gram of sorbent using Equation (5).

$$N_{CO_2} = \int_0^{t1} (F_{CO_2, tot} - F_{CO_2, t})dt$$

(4)

$$\% \text{ Capacity} = \left[\frac{\text{g } CO_2}{\text{g calcined sorbent}} \right] \times 100$$

(5)

Here, $F_{CO2,tot}$ represents the average value of CO_2 flow rate during the course of the conventional water gas shift reaction, $F_{CO2,t}$ represents the CO_2 flow rate at time t and t_1 represents the time point where the CO_2 content in the gas effluent did not increase any more after the breakthrough started.

Finally, a thermodynamic analysis of the SEWGS process has been conducted under different reaction conditions. The equilibrium compositions were obtained by minimizing the total Gibbs free energy of the reaction system. Aspen Plus 7.2 software (Aspentech) was used for calculations. The R-Gibbs reactor was specified as the reaction system, where the Peng-Robinson property method predicts the thermodynamic behavior of the system. According to the obtained results for the equilibrium prediction under sorption enhanced conditions, the present species at concentrations higher than 10^{-4} mol % were H_2, CO, CO_2, CH_4, H_2O, CaO and $CaCO_3$. Ethane, ethylene, acetylene and solid carbon (graphite) were also included in the product pool, but their concentrations in the equilibrium stream were not great enough to be considered as effective products. Product mole fractions are given on a dry basis.

3. Results and Discussion

3.1. Sorption-enhanced water gas shift process

A typical profile of gas product composition as a function of time on stream after the experimental SEWGS reaction process on 1%Pd/20%Ni-20%Co at 425 ºC is shown in Fig. 2. The evolution of the gas effluent compositions in the sorption enhanced process can be typically divided in three stages: pre-breakthrough, breakthrough and post-breakthrough [45,50,51]. During the pre-breakthrough stage, the calcined dolomite effectively captured CO_2 and thereby its concentration was very low (0.01 mol %). At

the same time, the WGS reaction was shifted towards the product side by the CO_2 removal and H_2 concentration was increased to high efficiency (99.28 mol %), whereas CO concentration was below the detection limit of the Micro GC and CH_4 concentration (0.70 mol %) was low. In the breakthrough region, the CaO sorbent became saturated, which was indicated by a rapid rise in CO_2 concentration and a reduction in the H_2 concentration. In the post-breakthrough region, the CO_2 capture by the sorbent was negligible and conventional WGS reaction (without CO_2 removal) was assumed to occur. The corresponding H_2 concentration was considerably lower than that during the active CO_2-capture stage. These results demonstrated that dolomite as CaO-based solid CO_2 acceptor is suitable for SEWGS, which effectively removed the CO_2 during the reaction and thus enhanced the performance of WGS for hydrogen production.

3.2. Effect of reaction temperature on SEWGS

Temperature is an important parameter in the SEWGS process, since it influences not only the thermodynamic equilibrium of carbonation and WGS reactions but also the rate of the reactions. The SEWGS reaction was conducted at different temperatures at a steam/CO ratio of 4 (CO pressure of 12.5 kPa) on 1%Pd/20%Ni-20%Co HT. The results are summarized in Table 1 together with the corresponding equilibrium compositions. It should be mentioned that an induction period before the SEWGS reaction was observed using a CO pressure of 12.5, which will be discussed later. The steady-state composition after the induction period was taken for the calculation of the concentrations listed in Table 1.

The equilibrium compositions obtained from the thermodynamic calculation (Table 1) showed that the hydrogen concentration decreases and the concentrations of methane,

CO and CO_2 increase concurrently with increasing the operating temperature. The results are in good agreement with those obtained in the sorption enhanced steam reforming of ethanol [45], as well as glucose and sorbitol [50]. At steam/CO ratio of 4, the CH_4 equilibrium concentration was only slightly increased with the temperature. In general, the experimental gas compositions from the SEWGS reaction were found to be rather consistent with the predicted equilibrium values. However, it should be noticed that the experimental CO_2 contents are slightly, but systematically lower than the equilibrium ones at different temperatures. It can be possibly ascribed to a possible deviation of thermodynamic properties of dolomites from the pure CaO used in the calculations. As a result, it possibly also caused slightly higher experimental concentrations of hydrogen at 500 ℃ and 525 ℃ compared to equilibrium ones. Anyhow, such deviations are within the experimental error range. In addition, the CO concentrations at 450-500 ℃ were lower than the equilibrium ones, which are also most likely within the experimental error. The CO concentration at 475 and 500 ℃ was below the GC detection limit.

The experimental results from the SEWGS reaction at CO pressure of 12.5 kPa (Table 1) indicated that the combination of CO_2 capture and WGS reaction yielded a high-purity hydrogen stream (> 99%) with low CO concentration. However, as mentioned above, the extent of the shift from the equilibrium composition was higher at low temperatures. The CO concentration increased concurrently with decreasing temperature from 475 ℃ to 425 ℃, while the CO_2 concentration was similar, which could be caused by a lower WGS catalyst activity at lower temperatures. The experimental methane content showed a high dependence on the temperature, which is different from the equilibrium results. The results showed CH_4 content decreased with

increasing temperature up to 500 ºC. As a consequence the H_2 content increased. It could be result of the unfavorable thermodynamics of the methanation reaction, enhanced WGS and methane reforming, as well as carbonation reaction for more effective removal of CO_2 inside the reactor [52], at higher temperatures. The observation is consistent with that found in SESR of ethanol where the larger deviation of the experimental H_2 contents from the corresponding equilibrium values was found at lower temperatures (500-525 ºC) due to higher CH_4 content in the gas product [45]. However, CH_4 concentration increased and H_2 content decreased with further increasing temperature from 500 ºC (Table 1), which is consistent with the increase in CO_2 content. The experimental results at higher temperatures are in good agreement with the thermodynamic prediction. Carbonation of CaO is less favorable at higher temperatures, which decreased the sorption enhancement on WGS and increased CO concentration, which led to enhanced methanation. It can be therefore concluded that hydrogen production by SEWGS is kinetically limited by the WGS reaction and enhanced methanation at lower temperatures (425-475 ºC), while it is thermodynamically unfavorable by the CO_2 capture at higher temperatures (475-550 ºC) due to reduced sorption enhancement for hydrogen production. There is a minimum CH_4 content (0.01%) and maximum hydrogen content (99.93%) at the optimized temperature of 500 ºC.

Since CO concentrations found in the product gas at 425 and 450 ºC were higher than expected and they deviated from the equilibrium values, two additional SEWGS experiments were performed under the same operating conditions at temperatures of 425 and 450 ºC, but using a lower CO partial pressure in the feed stream (6.25 kPa), in order to check if the CO concentration in the product gas at low temperature was

affected by the CO partial pressure. The H_2O partial pressure in the feed stream was decreased accordingly to maintain the steam/CO ratio of 4. It can be noted (Table 1) that at relatively low partial pressure of CO it was possible to fully convert CO until values below the detection limit of the Micro GC with high hydrogen purity at low temperatures. The results indicated that partial pressure of the reactants in the feed stream affected the product composition, which will be further investigated in the next section.

3.3. Effect of the steam/CO ratio and CO partial pressure in feed gas on SEWGS

Steam is often added beyond stoichiometric limit in reforming processes in order to promote hydrogen productivity and to prevent coking. The steam/CO ratio can have a significant impact on the hydrogen production by the SEWGS process. In the present study, the SEWGS reaction was conducted at different steam/CO ratios and CO partial pressures at 425 ºC, and the results are summarized in Table 2, together with the corresponding equilibrium compositions. The H_2O partial pressure in the feed stream (P_{H2O}) was changed accordingly to the CO partial pressure values in order to maintain the corresponding steam/CO ratio in each experiment, their values being also shown in Table 2 in parentheses.

The steam/CO ratio is expected to have an effect on the gas product composition, since an increase in steam concentration favors hydrogen production by shifting the equilibrium of WGS reaction. The thermodynamic analysis predicts only a slight decrease in hydrogen content from 99.98 to 99.80% with decreasing steam/CO ratio from 4 to 2, besides a methane content increase from 0.011 to 0.197%. Taking into account the experiments carried out with low CO partial pressure in the reactant mixture

(6.25 kPa), the H_2 purity obtained at steam/CO ratio of 2, 3 and 4 showed high values (98.6-99.3%), whereas a nearly complete conversion of CO was only found at steam/CO ratios of 3 and 4. When the steam/CO ratio was reduced to 2, a low CO content (0.01%) was found in the gas product. On the other hand, when the experiments were performed using higher CO partial pressure values in the reactant mixture (15.15-21.74 kPa), the hydrogen purity decreased compared to that obtained with low CO partial pressure at all the steam/CO ratios studied, the CO content in the gas product being very high. CO_2 content was kept almost unchanged regardless to the CO pressure and steam/CO ratio, with a value rather close to the equilibrium one, which indicated that the carbonation reaction of CaO occurred under the conditions studied in Table 2. Therefore, the results clearly indicated that an increase in CO partial pressure in the feed stream produces a negative effect on the CO conversion rate, namely negative apparent reaction order of CO. More importantly, this finding points out a challenge for SEWGS at high pressures in terms of catalyst activity at high CO partial pressure, suggesting that more active catalysts are highly desired.

Results also suggested that catalyst activity was high enough by performing the SEWGS reaction close to the equilibrium at CO partial pressure of 6.25 kPa with a space velocity WHSV= 3.44 h^{-1} and low temperature (425 ºC). However, the catalyst activity seems to be significantly reduced at high CO pressure (12.5 kPa) and low temperature. Results suggested that the gas composition was determined kinetically but not thermodynamically. It indicates that a more extensive study of the SEWGS process at high CO pressure values could be useful to provide kinetic information of the catalysts. Under high CO pressure conditions, as steam/CO ratio decreased, a strong decrease was also observed in the H_2 and CO contents, while a significant increase was

observed in the CH$_4$ content. Thus, very high methane concentration (10.24%) was found at steam/CO of 2. High CO pressure and low steam/CO ratio obviously enhanced methanation and decreased methane steam reforming simultaneously. He et al. [46] carried out sorption enhanced steam reforming experiments of glycerol and also found lower hydrogen purity at low values of steam-to-glycerol ratio. The authors suspected that carbonaceous species were formed on the catalyst under such conditions, causing deterioration in the catalyst activity, which caused an increase in the methane content at the expense of the hydrogen production. The results highlighted that catalysts with low activity to methanation and high activity to methane steam reforming are required at low temperatures. Summarizing, the results indicated that the partial pressure of the reactants in the feed stream can influence the catalyst activity, and thus the product composition. High CO pressure suppressed catalyst activity not only for WGS but also for methane steam reforming. It can be noted that at relatively low partial pressure of CO it was possible to fully convert CO until values below the detection limit of the Micro GC with high hydrogen purity at low temperatures.

The results of SEWGS also will help us to understand why we could get very high hydrogen yield and very low CO content by sorption enhanced reforming of different hydrocarbons and biomass-derived oxygenates on our Ni-Co bimetallic catalysts [43,45,46]. The steam reforming and WGS form a sequential reaction, and a high activity of the bimetallic catalyst will keep CO at low concentrations in the gas phase and thus it will avoid the suppressing effects of the high CO concentrations. Ideally, steam reforming function and WGS function should be integrated to the highest extent. Therefore, catalyst with a high WGS activity is also essential for the sorption enhanced reforming reactions in order to get high yield of hydrogen.

3.4. Effect of the catalyst reduction on SEWGS

The use of a catalyst in several reaction-regeneration cycles may affect its activity. Ni-Co catalysts used in continuous cyclic operation usually suffer from a reversible deactivation due to the loss of active sites during the regeneration step by means of oxidation of Ni and Co with high concentrations of CO_2 or by the oxidative gases added, such as oxygen, forming the corresponding oxides. As a consequence, they require a reduction step before the next cycle. Catalysts that are easily reducible and less sensitive to oxidative treatments at high temperatures are highly desirable to simplify the process. For this purpose, Pd was selected as a promoter for the Ni-Co catalysts. The presence of Pd in the Ni-Co catalyst used in the present work could promote the rapid production of H_2 which would assist the catalyst reduction, avoiding a reduction step between cycles in sorption enhanced biomass gasification, as suggested by Fermoso et al. [42] in a previous work. The effect of using unreduced 1%Pd/20%Ni-20%Co HT catalyst on the SEWGS reaction was checked by the repetition of one of the experiments at CO partial pressure of 6.25 kPa after the sorbent regeneration but without the reduction step of the catalyst. Fig. 3 shows the gas product composition as a function of time on stream after the SEWGS reaction using reduced and unreduced 1%Pd/20%Ni-20%Co HT catalyst for comparison.

The results indicated that the hydrogen purity from the SEWGS process was not affected by the reduction of the catalyst (99.8 mol % with the reduced catalyst and 99.7 mol % with the unreduced one). However, in the case of the reduced catalyst, the complete conversion of CO was achieved, since during the SEWGS reaction CO concentration was below the detection limit of the Micro GC. However, when unreduced catalyst was used a notable CO concentration (around 0.02 mol %) was

detected during the SEWGS process. Therefore, in order to minimize the CO concentration in the gas product stream of the SEWGS process and obtain a high-purity hydrogen gas, the reduction of the catalyst between consecutive cycles of reaction is needed. However, it should be pointed out that the reduction of the Co-Ni catalysts has been significantly improved by the promotion of noble metals, such as Pd, which simplifies the process in order to be used in circulating fluidized bed reactors to produce hydrogen with a low amount of impurities. On the other hand, results indicate that the catalyst is crucial for obtaining high-purity hydrogen by SEWGS, which is consistent with the results reported by Ramkumar and Fan [24].

3.5. Effect of the catalyst composition on SEWGS

Since the CH_4 concentrations detected in the experiments carried out with high CO partial pressure values in the feed stream at low temperatures (Tables 1 and 2) were extremely high, one additional SEWGS experiment was performed at 450 ºC with an even higher CO partial pressure in the feed stream (20.0 kPa), without using inert gas in the inlet stream, in order to confirm the rigorous methanation effect on identical catalyst, 1%Pd/20%Ni-20%Co. The gas product composition from this experiment is presented in Table 3. The results again showed very high methane production (2.65%) together with a decrease in the hydrogen purity until 96 mol %, which indicates that methanation could become the main problem in the highly efficient SEWGS process for yielding high-purity H_2.

As it has been concluded in previous sections, catalyst plays a very important role on the SEWGS reaction. So, catalysts should be rationally designed to have high activity for WGS and methane steam reforming but low methanation activity, besides keeping

its stability. Ni- and Co-based catalysts are widely accepted as appropriate low-cost metal catalysts for steam reforming of hydrocarbons, since Ni has exhibited good performance by favoring C-C and O-H bonds rupture and Co has presented high selectivity to hydrogen in steam reforming reactions [43], but monometallic catalysts could not meet all the requirements. Bi- or multi-metallic catalysts can be the choice to improve the catalyst functionality and Ni-Co bimetallic catalysts could be a good option. A previous kinetic screening study over a series of Ni-Co HT catalysts with different Ni/Co ratios has been performed in our research group and it suggested that the lowest methane production keeping high WGS activity was obtained on 30%Ni-10%Co HT catalyst [47]. Moreover, noble metals are known to have high reforming and WGS activity and good resistance to coke formation, although the high cost limits their applications. In the present work, Pd has been added in a relative low loading as the third metal to the Ni-Co catalyst. Three catalysts were selected in the present work for the evaluation of effects of the metal composition on SEWGS, namely 1%Pd/20%Ni-20%Co HT, 20%Ni-20%Co and 30%Ni-10%Co.

The results (Table 3) showed that the methane concentration in the product gas from the SEWGS reaction was much lower on 30%Ni-10%Co catalyst as compared to 1%Pd/20%Ni-20%Co catalyst, whereas methanation activity was notably increased on 20%Ni-20%Co catalyst. These results showed an improved capacity of the 30%Ni-10%Co catalyst for controlling the methanation reaction during the SEWGS, suggesting its lower methanation activity. Compared to the results obtained on 20%Ni-20%Co HT catalyst, the addition of Pd, i.e. 1%Pd/20%Ni-20%Co HT catalyst, increased the hydrogen purity and decreased the methane content (Table 3). Our kinetic study of the WGS reaction without sorption enhancement [47] illustrated a slight enhancement of

the methanation reaction by the Pd promoter in the Ni-Co catalysts. The observation of the decrease in methane concentration and increase in hydrogen concentration during SEWGS on Pd modified catalysts is thus mainly a result of enhanced methane steam reforming activity by Pd addition. These results again illustrated the importance of the catalysts in the SEWGS reaction and confirmed the necessity of an adequate strategy for a rational design of catalysts.

However, it should be mentioned that the catalyst composition has not been optimized for SEWGS in the present work. Wheeler et al. [38] have indicated a reaction rate order of Ni>Ru>Rh>Pt>Pd for high-temperature WGS (300-1000 ºC). Panagiotopoulou et al. [53] studied the methanation reaction of CO over supported noble metal catalysts (Ru, Rh, Pt and Pd) in the presence and absence of water, showing that the methanation activity of Rh and Ru is much higher than one on Pt and Pd catalysts. However, the selectivity to WGS in the presence of water followed the order Pt>Pd>Rh>Ru [53]. Jones et al. [54] studied the steam methane reforming on different transition metal catalysis and found an activity order of Ru~Rh>Ni~Ir~Pt~Pd. Analysis of the reported rate orders points out that Pt and Pd are potential promoters for the Ni-Co catalysts to achieve high activity of WGS and steam methane reforming but low activity for the methanation reaction. In addition to Pd, Pt-30%Ni-10%Co could be an attractive candidate for SEWGS.

3.6. Effect of hydrogen addition

During the sorption-enhanced WGS experiments carried out with high partial pressure of CO, a slow CO reaction rate at the beginning of the experiment was observed, which resulted in an induction period and a longer time to attain the lowest CO concentration

with the maximum production of hydrogen. This phenomenon was more notably observed using 20%Ni-20%Co HT catalyst (Fig. 4). In the case of the experiments carried out with low partial pressure of CO, this delay in the CO consumption was not observed and a very short time was taken to get the maximum conversion, as can be seen in Fig. 3 for the reduced 1%Pd/20%Ni-20%Co HT catalyst. A possible explanation for the initial slow reaction rate is that at the beginning of the experiment with high partial pressures of CO, the catalyst surface is strongly bonded and mostly occupied by carbon monoxide, thus hindering the shift reaction. Once the hydrogen emerges as a result of the WGS reaction, the catalyst surface is also occupied by the product gases including hydrogen and the reaction rate increases.

To confirm this assumption, an additional experiment was conducted in which a small amount of hydrogen was fed in the reactant stream. This experiment was carried out using 20%Ni-20%Co HT catalyst, since it was found to be less active at the beginning of the experiment. The reaction conditions were the same as described above but adding 20 mL min^{-1} of H$_2$ (P$_{H2}$=19.51 kPa) in the feed stream. Fig. 4 shows the CO concentration in the product gas as a function of time on stream after the SEWGS for this experiment compared to the CO concentrations obtained using the same catalyst without the addition of H$_2$ in the feed stream. The results showed that not only the reaction rate was enhanced by the addition of H$_2$ in the inlet stream, but also complete conversion of CO was achieved after 20 min on stream. A CO concentration below the detection limit of the Micro GC was not observed in the experiment performed without hydrogen addition. Hence, it could be concluded that a slow reaction rate of CO at the beginning of the SEWGS experiments with high CO partial pressure can be improved by the addition of a small amount of hydrogen to the reactant stream. In addition, high

concentration of surface hydrogen on the catalyst is speculated to greatly lower the coking potential [45,46].

3.7. Highly pure hydrogen production by SEWGS using a novel mixed oxide (CaCeZr) CO_2 sorbent and 30%Ni-10%Co HT catalyst

Since it has been well established in the literature that dolomite loses its CO_2 capture capacity over a number of cycles, the stability of the sorbent material can be considered one of the key challenges in the development of the SEWGS technology. Consequently, the choice of an adequate sorbent can be very important to generate a constant stream of pure hydrogen by the SEWGS process. An attempt to address this issue was made in the present work by synthesizing a mixed oxide material to be used as CO_2 sorbent, CaCeZr (10:1:1), whose cyclic stability under relatively high CO partial pressure conditions was tested in the SEWGS process. A sequence of six carbonation/decarbonation cycles in the SEWGS reaction was run. Fig. 5 shows the gas product composition as a function of time on stream after the first cycle of carbonation/decarbonation in the SEWGS process using CaCeZr as sorbent material. After the first cycle of carbonation/decarbonation, the effluent gas concentration profile showed a stream with highly pure hydrogen (99.8 mol %), CO concentration of 0.02 mol % and CH_4 content of 0.16 mol %.

The results of the successive cycles revealed that the H_2 concentration in the gas product remained quite constant over the period of 6 cycles (around 99.8 mol %), methanation reaction was observed to be reduced as the number of cycles proceeded from ca. 0.16 to 0.003 mol %, whereas the unconverted CO decreased until 0.01 mol %. However, the time of the pre-breakthrough stage was reduced as the number of cycles proceeded. Fig. 6 shows the in situ CO_2 capture capacity of the calcined CaCeZr (10:1:1) sorbent

during six cycles of SEWGS reaction. Despite the good capacity of the mixed oxide sorbent in the initial cycles, its CO_2 capture capacity decreased during the first three cycles, but after that it appeared to be stabilized. In contrast, a continued decline in the CO_2 capture capacity has been reported for dolomite sorbent. The CO_2 capture capacity of CaCeZr sorbent was found to be 0.378 g CO_2/g sorbent during the first cycle, which is comparable, although slightly lower, to that reported in previous works with a similar sorbent by Sultana and Chen [49] under sorption enhanced steam methane reforming at 570 °C and for ethanol steam reforming at 575 °C. The SEWGS experiments carried out in the present study with dolomite as sorbent material showed that the CO_2 capture capacity of dolomite was 0.26 and 0.23 g CO_2/g sorbent during the first and second cycles of reaction, respectively. The comparison of the initial capture capacity between the dolomite and the mixed oxide sorbent indicated that the CaCeZr (10:1:1) sorbent had a higher CO_2 capture capacity during the first cycle of SEWGS reaction than dolomite under these SEWGS conditions. Since the capture capacity of the dolomite is known to deteriorate during multiple cycle operation, it can be concluded that the CaCeZr (10:1:1) sorbent could show a better stability in sorption enhanced processes.

The reason for the relatively lower CO_2 capture capacities under SEWGS reaction conditions as compared to those of sorption enhanced reforming in the previous work [49] could be the difference in reactivity as the two reaction proceed. As indicated above, under the conditions of the present SEWGS reaction study, CO reacts with an initial slow reaction rate, so possibly a lower amount of CO_2 is generated in the reaction zone as compared to that produced during the steam methane reforming process. The capture capacity of the sorbent is also a function of the CO_2 partial pressure and hence highly depends on the amount of CO_2 generated in the reaction zone. A slow initial

production of CO_2 could result in a low capture capacity under the SEWGS conditions investigated as compared to the reforming process. Finally, it can be deduced that the use of the CaCeZr mixed oxide sorbent together with an appropriate WGS catalyst could for the first time allow stable production of highly pure hydrogen, in particular fuel-cell grade hydrogen, at low CO pressures by cyclic SEWGS process.

In order to understand the mechanism of the observed deactivation of sorbents, the characterization of both fresh and spent catalyst (10%Co-30%Ni) and sorbent material (CaCeZr 10:1:1) were performed by means of XRD and BET surface area measurements. The XRD spectra of the fresh calcined sorbent is shown in Fig. 7. The XRD pattern indicates the presence of CaO and $Ce_{0.5}Zr_{0.5}O_2$ phases in a well-crystalline structure of the sorbent material. The BET surface area of the calcined sorbent was found to be 31.2 $m^2\,g^{-1}$ and pore volume of 0.14 $cm^3\,g^{-1}$ (Table 4).

The XRD analysis of the fresh 10%Co-30%Ni HT catalyst (Fig. 8) shows prominent 2θ peaks at about 11.5, 23.1, 34.9, 39.3, 46.8 and 62.1°, characteristic for hydrotalcites [43], i.e. with the general pattern of sharp, symmetric and intense lines at low values of 2θ angle and relatively less intense and asymmetric lines at higher angular values. The XRD spectra of the calcined catalyst sample (Fig. 9) shows that there is no residual hydrotalcite structure due to the loss of water and carbon dioxide from the anionic interlayer of hydrotalcite precursors and the presence of poorly crystallized mixed oxide phases. The peaks in the XRD pattern correspond to the possible presence of NiO, Co_3O_4, $CoAl_2O_4$, $NiCo_2O_4$, $MgAl_2O_4$ and $MgNiO_2$ phases, which are however impossible to be distinguished due to heavy overlaps. The BET surface area and pore volume of the calcined catalyst were found to be 175 $m^2\,g^{-1}$ and of 0.6 $cm^3\,g^{-1}$, respectively (Table 4).

After completion of seven cycles of SEWGS, it was difficult to separate the catalyst and the sorbent from the catalyst/sorbent mixture. Therefore, the XRD and BET analyses of the sorbent/catalyst (20/1 g/g) mixture were done in order to evaluate the changes in the physical-chemical properties. The XRD pattern is shown in Fig. 10, which indicates the presence of CaO, $Ce_{0.5}Zr_{0.5}O_2$ and $CaZrO_3$ from the sorbent, whereas Ni-containing oxides (NiO, MgO and Ni-Mg oxides) are identified from the catalyst. The catalyst did not transfer back to hydrotalcite structure during the cycles. The average crystal sizes have been estimated from the XRD peaks using Scherrer equation, which are summarized in Table 4. The results show a slight increase in CaO crystal of sorbent from 40 nm to 49 nm after seven cycles. Similarly, the average crystallite size of $Ce_{0.5}Zr_{0.5}O_2$ increased from 10 nm to 16 nm. The new phase $CaZrO_3$ formed showed a crystal size of 32 nm. In the case of the catalyst, XRD results showed a strong growth in the Ni-containing oxides crystal from 3.8 nm to 24 nm after seven cycles. The crystal size of Ni-containing oxides has been estimated by considering the XRD peak at 2θ value of ca. 44°.

The initial average surface area of the catalyst/sorbent mixture was calculated to be 38 $m^2\ g^{-1}$, whereas it was reduced to 12 $m^2\ g^{-1}$ after seven cycles (Table 4). Similarly the pore volume of the mixture was reduced from 0.16 $cm^3\ g^{-1}$ to 0.05 $cm^3\ g^{-1}$ after seven cycles of SEWGS. Obviously, the surface area of catalysts and sorbents significantly decreased after cycles. We previously reported [55] that the surface area of hydrotalcite-derived supports decreased from about 200 $m^2\ g^{-1}$ to 20-30 $m^2\ g^{-1}$ after more than 50 hours under steam reforming reaction at 630 ºC and 20 bars, whereas Ni particles were relatively stable and Ni dispersion decreased about 20%. In addition, regeneration of the sorbents at high temperature could also cause sintering of catalysts and sorbents,

resulting in an irreversible deactivation. It should be mentioned that the Ni-Co catalysts were calcined at a relatively low temperature (600 ºC) in the present work, which was optimized to get a high Ni dispersion but not optimized for the SEWGS reaction, where a high temperature (750 ºC) is required for the regeneration of the sorbents. This fact recommends a high temperature (>750 ºC) for calcination of catalysts in future works.

The surface area of the sorbents must have been also reduced by cycling operation of SEWGS, since the crystal size of CaO and $Ce_{0.5}Zr_{0.5}O_2$ increased, and a new phase of $CaZrO_3$ with a relatively large crystal size was formed. It has been also demonstrated in the literature that the presence of steam could have deactivated the Ca-containing mixed oxide sorbents during cycles due to sintering [56,57]. Taking into account the stable H_2, CH_4 and CO contents during the SEWGS cycles, the observed decrease in the CO_2 capacity (Fig. 5) will be mainly result of the deactivation of the sorbent due to the BET surface area decrease, the CaO sintering and the loss of CaO active material by formation of $CaZrO_3$.

4. Conclusions

The integration of in-situ CO_2 capture to the water gas shift reaction, i.e. sorption-enhanced water gas shift (SEWGS) process, have been investigated to effectively produce a highly hydrogen-rich gas stream in a single step. The experimental results and the thermodynamic analysis showed that incorporating in-situ CO_2 capture into the water gas shift reaction is essential to achieve a one-step high yield of hydrogen. The SEWGS reaction for hydrogen production was studied in a fixed-bed reactor using 1%Pd/20%Ni-20%Co HT catalyst and calcined dolomite as CO_2 sorbent. Ni-Co catalysts and a novel CaCeZr mixed oxide as sorbent were also studied. We clearly

28

illustrated that the catalyst plays a significant role in the one-step hydrogen production by SEWGS. The 1%Pd/20%Ni-20%Co HT catalyst was found to be the most active for attaining the complete CO conversion, but it was associated with significant methanation when low temperatures and high CO partial pressures in the feed stream were used, which was also detected with the use of 20%Ni-20%Co HT catalyst. The results indicated that methanation reaction increased strongly with increasing CO partial pressure in the feed stream. The utilization of 30%Ni-10%Co HT catalyst was proved to be the best option for the studied SEWGS process due to the reduced methanation reaction at low temperatures using high CO partial pressures in the feed stream. Furthermore, the synthesized CaO-based mixed oxide, CaCeZr, sorbent could be a good option for using in SEWGS reaction due to its stability and capture capacity.

There is an optimized temperature for hydrogen production by the SEWGS reaction. The hydrogen production by SEWGS is kinetically limited by the WGS reaction at low temperatures (425-475 °C), while it is thermodynamically unfavorable at high temperatures (475-550 °C). The concentration of hydrogen from SEWGS reaction was higher than 99.8 mol % between 450-525 °C, steam/CO ratio of 4 and CO partial pressure of 12.5 kPa using 1%Pd/20%Ni-20%Co HT catalyst and dolomite as sorbent. The lowest CO concentration was found at temperatures of 475-500 °C, whereas the methanation reaction was effectively reduced at temperatures higher than 500 °C. Under the conditions of the present study, a maximum hydrogen concentration of 99.93% together with a very low CH_4 concentration (0.01 mol %) and negligible CO content (below the detectable limit of the Micro GC analyzer) was obtained after the SEWGS reaction at 500 °C, steam/CO of 4 and CO partial pressure of 12.5 kPa. Such a low level of CO might allow the direct use of the gas product in low-temperature proton exchange

membrane (PEM) fuel cells without subsequent CO removal. Under these conditions, the reduction of the 1%Pd/20%Ni-20%Co HT catalyst between successive SEWGS cyclic reactions was proved to be necessary in order to reach full CO conversion. On the other hand, the slow reaction rate found in the preliminary stage of reaction with high partial pressure of CO in the feed stream can be overcome by the addition of hydrogen in the inlet stream, which not only significantly enhanced the rate of shift reaction but also resulted in the complete conversion of CO.

The major potential advantages of the studied process are the production of a high-purity hydrogen stream from water gas shift reaction in a single step and the possibility of obtaining a fuel-cell grade hydrogen gas with a low enough CO concentration. However, future works studying the activity and stability of the catalysts over an increased number of cycles under high CO and steam partial pressure conditions would be still necessary. Also, the addition of Pd to the 30%Ni-10%Co HT catalyst should be tested, since it could potentially incorporate significant advantages in relation to the improvement in the CO conversion and reduction of methanation reaction during the SEWGS process.

References

[1] R. Gupta, K. Pant, Hydrogen Fuel – Production, Transport, and Storage, CRC Press Taylor & Francis Group, 2009.

[2] J.D. Holladay, J. Hu, D.L. King, Y. Wang, Catal. Today 139 (2009) 244-260.

[3] T. Chapman, Physics World, 2002.

[4] C. Ratnasamy, J.P. Wagner, Cat. Rev. - Sci. Eng. 51 (2009) 325-440.

[5] C. Rhodes, B. Peter Williams, F. King, G.J. Hutchings, Catal. Commun. 3 (2002) 381-384.

[6] M.V. Twigg, Catalyst handbook, 2nd ed., Manson Publishing, London, 1996.

[7] A.F. Ghenciu, Curr. Opin. Solid State Mater. Sci. 6 (2002) 389-399.

[8] T.V. Choudhary, D.W. Goodman, Catal. Today 77 (2002) 65-78.

[9] H.-J. Ryu, S.-H. Jo, Y.C. Park, C.-K. Yi, Reaction characteristics of two water gas shift catalysts in a bubbling fluidized bed reactor for SEWGS process, The 13th International Conference on Fluidization - New Paradigm in Fluidization Engineering, 2010.

[10] N.A. Koryabkina, A.A. Phatak, W.F. Ruettinger, R.J. Farrauto, F.H. Ribeiro, J. Catal. 217 (2003) 233-239.

[11] D.P. Harrison, Ind. Eng. Chem. Res. 47 (2008) 6486-6501.

[12] L. Barelli, G. Bidini, F. Gallorini, S. Servili, Energy 33 (2008) 554-570.

[13] D. Chen, L. He, ChemCatChem 3 (2011) 490-511.

[14] C.R. Müller, R. Pacciani, C.D. Bohn, S.A. Scott, J.S. Dennis, Ind. Eng. Chem. Res. 48 (2009) 10284-10291.

[15] R.W. Stevens Jr, A. Shamsi, S. Carpenter, R. Siriwardane, Fuel 89 (2010) 1280-1286.

[16] P.D. Cobden, P. van Beurden, H.T.J. Reijers, G.D. Elzinga, S.C.A. Kluiters, J.W. Dijkstra, D. Jansen, R.W. van den Brink, Int. J. Greenh. Gas Control 1 (2007) 170-179.

[17] Z. Yong, V. Mata, A.r.E. Rodrigues, Sep. Purif. Technol. 26 (2002) 195-205.

[18] H.M. Jang, K.B. Lee, H.S. Caram, S. Sircar, Chem. Eng. Sci. 73 (2012) 431-438.

[19] M.G. Beaver, H.S. Caram, S. Sircar, Int. J. Hydrogen Energy 34 (2009) 2972-2978.

[20] E. Ochoa-Fernández, C. Lacalle-Vilà, T. Zhao, M. Rønning, D. Chen, in: M.S. Fábio Bellot Noronha, S.-A. Eduardo Falabella (Eds.), Stud. Surf. Sci. Catal., Elsevier, 2007, pp. 159-164.

[21] W. Gluud, K. Keller, R. Schonfelder, W. Klempt, Production of Hydrogen, U.S. Patent 1816523, 1931.

[22] C. Han, D.P. Harrison, Chem. Eng. Sci. 49 (1994) 5875-5883.

[23] L. He, D. Chen, ChemSusChem 3 (2010) 1169-1171.

[24] S. Ramkumar, L.-S. Fan, Energy Fuels 24 (2010) 4408-4418.

[25] G. Wu, C. Zhang, S. Li, Z. Huang, S. Yan, S. Wang, X. Ma, J. Gong, Energy Environ. Sci. 5 (2012) 8942-8949.

[26] B. Dou, G.L. Rickett, V. Dupont, P.T. Williams, H. Chen, Y. Ding, M. Ghadiri, Bioresour. Technol. 101 (2010) 2436-2442.

[27] K. Johnsen, J.R. Grace, S.S.E.H. Elnashaie, L. Kolbeinsen, D. Eriksen, Industrial & Engineering Chemistry Research 45 (2006) 4133-4144.

[28] A. Silaban, M. Narcida, D.P. Harrison, Chem. Eng. Commun. 146 (1996) 149-162.

[29] M. Kato, S. Yoshikawa, K. Nakagawa, J. Mater. Sci. Lett. 21 (2002) 485-487.

[30] M.A. Escobedo Bretado, M.D. Delgado Vigil, J.S. Gutiérrez, A. López Ortiz, V. Collins-Martínez, Int. J. Hydrogen Energy 35 (2010) 12083-12090.

[31] M.A. Escobedo Bretado, M.D. Delgado Vigil, V.H. Collins-Martinez, A. López Ortiz, Int. J. Chem. React. Eng. 6 (2008) 1542-6580.

[32] N.H. Florin, J. Blamey, P.S. Fennell, Energy & Fuels 24 (2010) 4598-4604.

[33] J. Mastin, A. Aranda, J. Meyer, Energy Procedia 4 (2011) 1184-1191.

[34] H.A.J. van Dijk, S. Walspurger, P.D. Cobden, D. Jansen, R.W. van den Brink, F.G. de Vos, Energy Procedia 1 (2009) 639-646.

[35] S.S. Hla, D. Park, G.J. Duffy, J.H. Edwards, D.G. Roberts, A. Ilyushechkin, L.D. Morpeth, T. Nguyen, Chem. Eng. J. 146 (2009) 148-154.

[36] S. Natesakhawat, X. Wang, L. Zhang, U.S. Ozkan, J. Mol. Catal. A: Chem. 260 (2006) 82-94.

[37] J.Y. Lee, D.-W. Lee, K.-Y. Lee, Y. Wang, Catal. Today 146 (2009) 260-264.

[38] C. Wheeler, A. Jhalani, E.J. Klein, S. Tummala, L.D. Schmidt, J. Catal. 223 (2004) 191-199.

[39] S. Hilaire, X. Wang, T. Luo, R.J. Gorte, J. Wagner, Appl. Catal. A-Gen 215 (2001) 271-278.

[40] K.-R. Hwang, C.-B. Lee, J.-S. Park, J. Power Sources 196 (2011) 1349-1352.

[41] Y. Schuurman, C. Marquez-Alvarez, V.C.H. Kroll, C. Mirodatos, Catal. Today 46 (1998) 185-192.

[42] J. Fermoso, F. Rubiera, D. Chen, Energy Environ. Sci. 5 (2012) 6358-6367.

[43] L. He, H. Berntsen, E. Ochoa-Fernández, J. Walmsley, E. Blekkan, D. Chen, Top. Catal. 52 (2009) 206-217.

[44] X. Hu, G. Lu, Appl. Catal. B-Environ. 88 (2009) 376-385.

[45] L. He, H. Berntsen, D. Chen, J. Phys. Chem. A 114 (2010) 3834-3844.

[46] L. He, J.M.S. Parra, E.A. Blekkan, D. Chen, Energy Environ. Sci. 3 (2010) 1046-1056.

[47] T. Noor, J. Zhu, J. Yang, D. Chen, (in preparation).

[48] E. Ochoa-Fernández, C. Lacalle-Vilà, K. Christensen, J. Walmsley, M. Rønning, A. Holmen, D. Chen, Top. Catal. 45 (2007) 3-8.

[49] K.S. Sultana, D. Chen, Catal. Today 171 (2011) 43-51.

[50] L. He, D. Chen, ChemSusChem 5 (2012) 587-595.

[51] J. Fermoso, L. He, D. Chen, Int. J. Hydrogen Energy 37 (2012) 14047-14054.

[52] E. Ochoa-Fernandez, M. Ronning, X. Yu, T. Grande, D. Chen, Industrial & Engineering Chemistry Research 47 (2008) 434-442.

[53] P. Panagiotopoulou, D.I. Kondarides, X.E. Verykios, Applied Catalysis A: General 344 (2008) 45-54.

[54] G. Jones, J.G. Jakobsen, S.S. Shim, J. Kleis, M.P. Andersson, J. Rossmeisl, F. Abild-Pedersen, T. Bligaard, S. Helveg, B. Hinnemann, J.R. Rostrup-Nielsen, I. Chorkendorff, J. Sehested, J.K. Nørskov, J. Catal. 259 (2008) 147-160.

[55] K.O. Christensen, D. Chen, R. Lødeng, A. Holmen, Applied Catalysis A: General 314 (2006) 9-22.

[56] R.H. Borgwardt, Chem. Eng. Sci. 44 (1989) 53-60.

[57] R.H. Borgwardt, Ind. Eng. Chem. Res. 28 (1989) 493-500.

Figure captions

Fig. 1. Schematic flow diagram of the experimental setup used for SEWGS experiments.

Fig. 2. Evolution of the product gas composition (dry basis; ◆ H_2; ● CO; ■ CH_4; ▲ CO_2) with time on stream during the SEWGS reaction. Reaction conditions: 425 ºC, 1 atm, steam/CO=4 mol/mol, sorbent/catalyst=25 g/g, CO partial pressure in the feed stream=6.25 kPa, H_2O partial pressure in the feed stream=25.00 kPa, WHSV=3.44 h^{-1}, calcined dolomite as sorbent and 1%Pd/20%Ni-20%Co HT catalyst.

Fig. 3. Evolution of the product gas composition with time on stream during the SEWGS reaction using reduced and unreduced 1%Pd/20%Ni-20%Co HT catalyst (dry basis; ◆ H_2-red; ● CO-red; ■ CH_4-red; ▲ CO_2-red; ◇ H_2-unred; ○ CO-unred; □ CH_4-unred; △ CO_2-unred). Reaction conditions: 425 ºC, 1 atm, steam/CO=4 mol/mol, WHSV=3.44 h^{-1}, sorbent/catalyst=25 g/g, CO partial pressure in the feed stream=6.25 kPa, H_2O partial pressure in the feed stream=25.00 kPa and calcined dolomite as sorbent.

Fig. 4. Evolution of the CO concentration in the product gas with time on stream during the SEWGS reaction using catalysts with different metal composition (dry basis; ● 1%Pd/20%Ni-20%Co HT and P_{CO}=15.15 kPa, P_{H2O}=60.61 kPa; ○ 20%Ni-20%Co HT and P_{CO}=15.15 kPa, P_{H2O}=60.61 kPa; ◖ 30%Ni-10%Co HT and P_{CO}=15.15 kPa, P_{H2O}=60.61 kPa; ◆ 20%Ni-20%Co HT and P_{CO}=12.20 kPa, P_{H2O}=48.78 kPa, P_{H2}=19.51 kPa). Reaction conditions: 450 ºC, 1 atm, steam/CO=4 mol/mol, WHSV=2.87 h^{-1}, sorbent/catalyst=15 g/g and calcined dolomite as sorbent.

Fig. 5. Evolution of the product gas composition with time on stream during the first cycle of carbonation/decarbonation in the SEWGS process using CaCeZr (10:1:1) as sorbent (dry basis; ◆ H_2; ● CO; ■ CH_4; ▲ CO_2). Reaction conditions: 450 ℃, 1 atm, steam/CO=4 mol/mol, WHSV=2.29 h^{-1}, sorbent/catalyst=20 g/g, CO partial pressure in the feed stream=14.29 kPa, H_2O partial pressure in the feed stream=57.14 kPa and 30%Ni-10%Co HT catalyst.

Fig. 6. In situ CO_2 capture capacity of calcined CaCeZr (10:1:1) sorbent during the first six cycles of SEWGS reaction. Reaction conditions: 450 ℃, 1 atm, steam/CO=4 mol/mol, WHSV=2.29 h^{-1} sorbent/catalyst=20 g/g, CO partial pressure in the feed stream=14.29 kPa, H_2O partial pressure in the feed stream=57.14 kPa and 30%Ni-10%Co HT catalyst.

Fig. 7. XRD pattern of calcined Ca:Ce:Zr (10:1:1) mix oxide sorbent, CaO (●), $Ce_{0.5}Zr_{0.5}O_2$ (◆).

Fig. 8. XRD pattern of uncalcined 30%Ni-10%Co hydrotalcite catalyst.

Fig. 9. XRD pattern of calcined 30%Ni-10%Co hydrotalcite catalyst. Peaks marked with (◇) are characteristic of NiO, MgO, $MgNiO_2$, Co_3O_4, $CoAl_2O_4$, $NiAl_2O_4$, $MgCo_2O_4$ and Al_2MgO_4.

Fig. 10. XRD pattern of CaCeZr (10:1:1) and 30%Ni-10%Co hydrotalcite catalyst after seven cycles of SEWGS. CaO (●), $Ce_{0.5}Zr_{0.5}O_2$ (◆) $CaZrO_3$ (△) NiO (○).

Table 1

Effect of temperature on product gas composition from SEWGS reaction. Reaction conditions: steam/CO=4 mol/mol, 1 atm, WHSV=6.88 h^{-1} (P_{CO}=12.50 kPa) and 3.44 h^{-1} (P_{CO}=6.25 kPa), sorbent/catalyst=10 g/g, calcined dolomite as sorbent and 1%Pd/20%Ni-20%Co HT catalyst.

Temperature [ºC]	Dry product gas composition [mol %]			
	H_2	CH_4	CO	CO_2
SEWGS experiments with P_{CO}=12.50 kPa and P_{H2O}=50.00 kPa				
425	99.05	0.91	0.04	0.004
450	99.84	0.15	0.004	0.004
475	99.77	0.23	n.d.[a]	0.004
500	99.93	0.01	n.d.[a]	0.06
525	99.84	0.05	0.04	0.07
550	99.63	0.01	0.04	0.31
Equilibrium				
425	99.98	0.011	0.0001	0.004
450	99.98	0.011	0.0005	0.011
475	99.96	0.011	0.002	0.030
500	99.91	0.010	0.005	0.075
525	99.80	0.010	0.014	0.177
550	99.56	0.009	0.036	0.397
SEWGS experiments with P_{CO}=6.25 kPa and P_{H2O}=25.00 kPa				
425	98.64	1.34	n.d.[a]	0.01
450	99.35	0.63	n.d.[a]	0.02
Equilibrium				
425	99.98	0.011	0.0001	0.004
450	99.98	0.011	0.0005	0.011

[a] n.d.: not detected.

Table 2

Effect of steam/CO ratio and CO partial pressure in the feed stream on product gas composition from SEWGS reaction. Reaction conditions: 425 ºC; 1 atm, WHSV=3.44 h^{-1}, sorbent/catalyst=10 g/g, calcined dolomite as sorbent and 1%Pd/20%Ni-20%Co HT catalyst.

Steam/CO	P_{CO} (P_{H2O}) [kPa]	Dry product gas composition [mol %]			
		H$_2$	CH$_4$	CO	CO$_2$
SEWGS experiments					
4	6.25 (25.00)	98.64	1.34	n.d.[a]	0.01
	15.15 (60.61)	96.06	3.17	0.75	0.01
3	6.25 (18.75)	99.26	0.70	n.d.[a]	0.02
	17.86 (53.57)	95.17	4.37	0.43	0.01
2	6.25 (12.50)	98.91	1.05	0.01	0.01
	21.74 (43.48)	89.57	10.24	0.13	0.04
Equilibrium					
4	6.25 (25.00)	99.98	0.011	0.0001	0.004
	15.15 (60.61)	99.98	0.011	0.0001	0.004
3	6.25 (18.75)	99.96	0.034	0.0002	0.003
	17.86 (53.57)	99.96	0.034	0.0002	0.003
2	6.25 (12.50)	99.80	0.197	0.0002	0.002
	21.74 (43.48)	99.80	0.197	0.0002	0.002

[a] n.d.: not detected.

Table 3

Effect of metal composition in the catalyst on product gas composition from SEWGS reaction. Reaction conditions: 450 ºC; 1 atm, steam/CO=4 mol/mol, WHSV=6.88 h^{-1} (P_{CO}=20.00 kPa) and 2.87 h^{-1} (P_{CO}=15.15 kPa), sorbent/catalyst=15 g/g and calcined dolomite as sorbent.

Catalyst	P_{CO} (P_{H2O}) [kPa]	Dry product gas composition [mol %]			
		H$_2$	CH$_4$	CO	CO$_2$
SEWGS experiments					
1%Pd/20%Ni-20%Co HT	20.00 (80.00)	95.73	2.65	1.61	0.02
1%Pd/20%Ni-20%Co HT	15.15 (60.61)	99.17	0.78	0.02	0.03
20%Ni-20%Co HT	15.15 (60.61)	98,27	2.13	0.03	0.03
30%Ni-10%Co HT	15.15 (60.61)	99.74	0.20	0.03	0.03
Equilibrium		99.98	0.011	0.0005	0.011

Table 4

Physical-chemical properties of catalyst (10%Co-30%Ni HT) and sorbent (CaCeZr) before and after SEWGS experiments.

Sample	XRD analysis	N$_2$ Sorption		
	Crystallite Size (nm)	BET surface area (m^{2}g^{-1})	Pore volume (cm^{3}g^{-1})	Pore diameter (nm)
Before SEWGS experiments				
30%Ni-10%Co HT	NiO (3.8)	175	0.6	11
CaCeZr	CaO (40)	31.2	0.14	---
	Ce$_{0.5}$Zr$_{0.5}$O$_2$ (10)			
After SEWGS experiments				
Catalyst and sorbent mixture	NiO (24)	12.1	0.05	15.9
	CaO (49)			
	Ce$_{0.5}$Zr$_{0.5}$O$_2$ (16)			
	CaZrO$_3$ (32)			

Fig. 1. Schematic flow diagram of the experimental setup used for SEWGS experiments.

Fig. 2. Evolution of the product gas composition (dry basis; ◆ H_2; ● CO; ■ CH_4; ▲ CO_2) with time on stream during the SEWGS reaction. Reaction conditions: 425 ℃, 1 atm, steam/CO=4 mol/mol, sorbent/catalyst=25 g/g, CO partial pressure in the feed stream=6.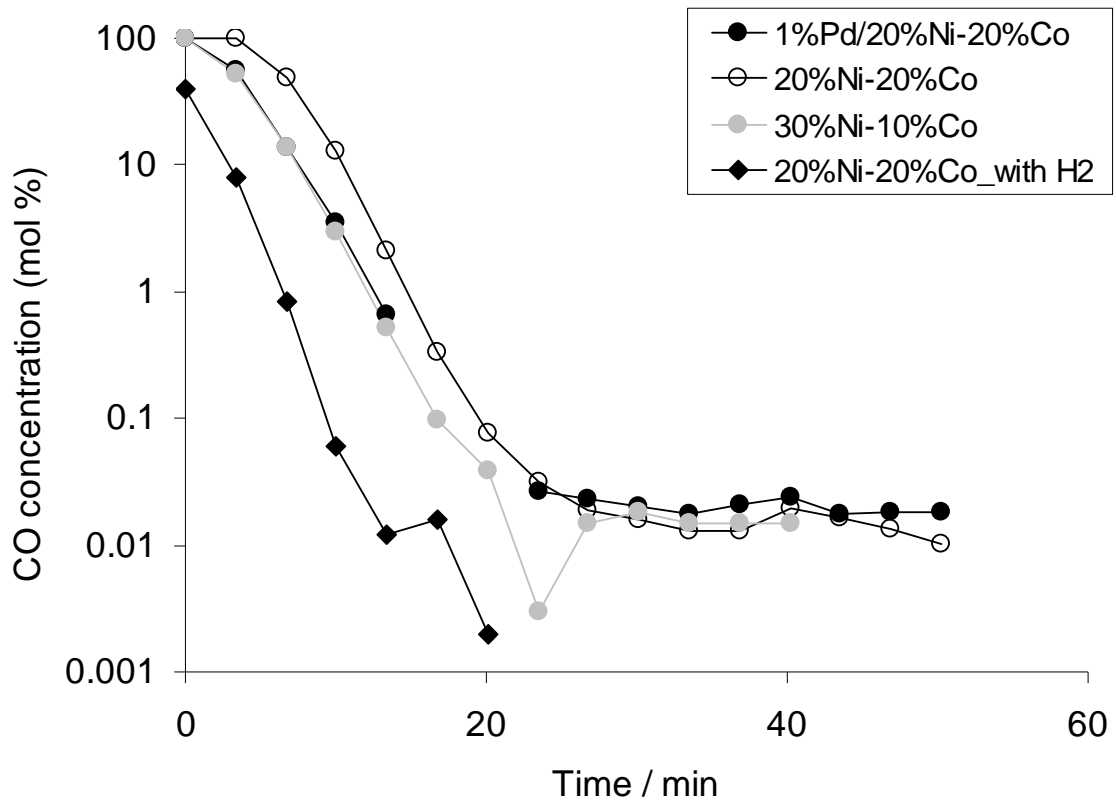25 kPa, H_2O partial pressure in the feed stream=25.00 kPa, WHSV=3.44 h^{-1}, calcined dolomite as sorbent and 1%Pd/20%Ni-20%Co HT catalyst.

Fig. 3. Evolution of the product gas composition with time on stream during the SEWGS reaction using reduced and unreduced 1%Pd/20%Ni-20%Co HT catalyst (dry basis; ◆ H_2-red; ● CO-red; ■ CH_4-red; ▲ CO_2-red; ◇ H_2-unred; ○ CO-unred; □ CH_4-unred; △ CO_2-unred). Reaction conditions: 425 ºC, 1 atm, steam/CO=4 mol/mol, WHSV=3.44 h^{-1}, sorbent/catalyst=25 g/g, CO partial pressure in the feed stream=6.25 kPa, H_2O partial pressure in the feed stream=25.00 kPa and calcined dolomite as sorbent.

Fig. 4. Evolution of the CO concentration in the product gas with time on stream during the SEWGS reaction using catalysts with different metal composition (dry basis; ● 1%Pd/20%Ni-20%Co HT and P_{CO}=15.15 kPa, P_{H2O}=60.61 kPa; ○ 20%Ni-20%Co HT and P_{CO}=15.15 kPa, P_{H2O}=60.61 kPa; ● 30%Ni-10%Co HT and P_{CO}=15.15 kPa, P_{H2O}=60.61 kPa; ◆ 20%Ni-20%Co HT and P_{CO}=12.20 kPa, P_{H2O}=48.78 kPa, P_{H2}=19.51 kPa). Reaction conditions: 450 ℃, 1 atm, steam/CO=4 mol/mol, WHSV=2.87 h^{-1}, sorbent/catalyst=15 g/g and calcined dolomite as sorbent.

Fig. 5. Evolution of the product gas composition with time on stream during the first cycle of carbonation/decarbonation in the SEWGS process using CaCeZr (10:1:1) as sorbent (dry basis; ◆ H_2; ● CO; ■ CH_4; ▲ CO_2). Reaction conditions: 450 ºC, 1 atm, steam/CO=4 mol/mol, WHSV=2.29 h^{-1}, sorbent/catalyst=20 g/g, CO partial pressure in the feed stream=14.29 kPa, H_2O partial pressure in the feed stream=57.14 kPa and 30%Ni-10%Co HT catalyst.
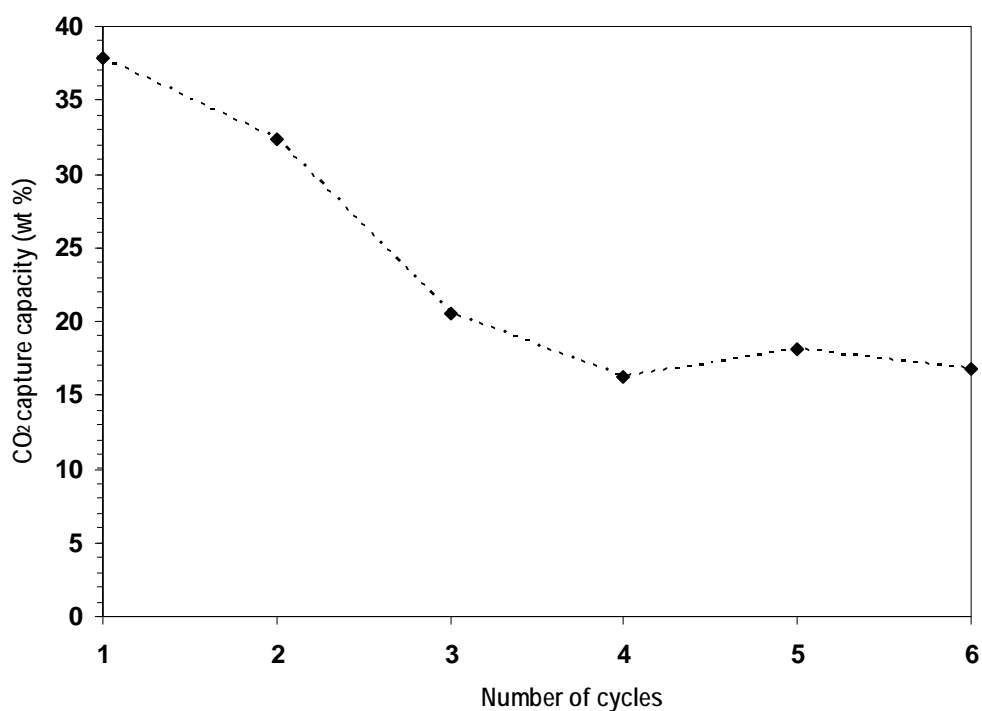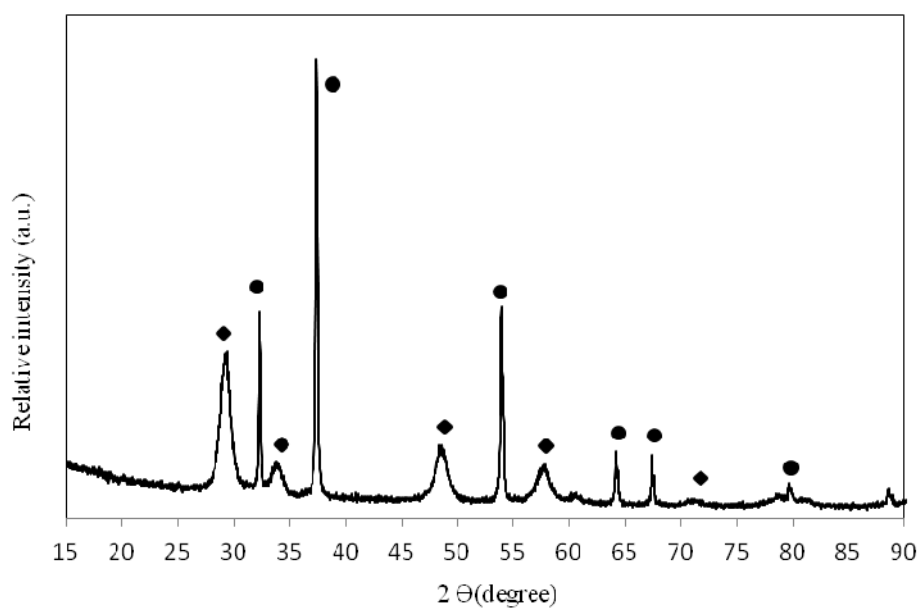
Fig. 6. In situ CO_2 capture capacity of calcined CaCeZr (10:1:1) sorbent during the first six cycles of SEWGS reaction. Reaction conditions: 450 ℃, 1 atm, steam/CO=4 mol/mol, WHSV=2.29 h^{-1} sorbent/catalyst=20 g/g, CO partial pressure in the feed stream=14.29 kPa, H_2O partial pressure in the feed stream=57.14 kPa and 30%Ni-10%Co HT catalyst.

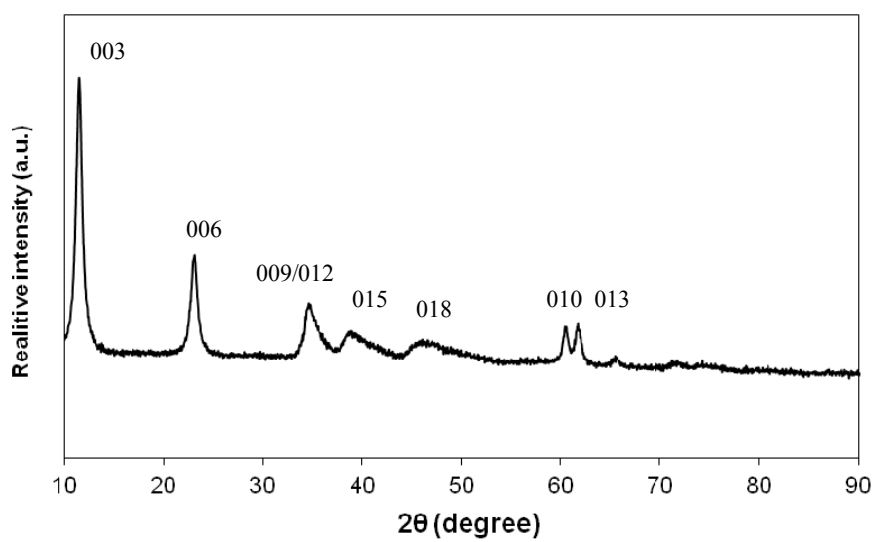**Fig. 7.** XRD pattern of calcined Ca:Ce:Zr (10:1:1) mix oxide sorbent, CaO (●), $Ce_{0.5}Zr_{0.5}O_2$ (◆).

Fig. 8. XRD pattern of uncalcined 30%Ni-10%Co hydrotalcite catalyst.

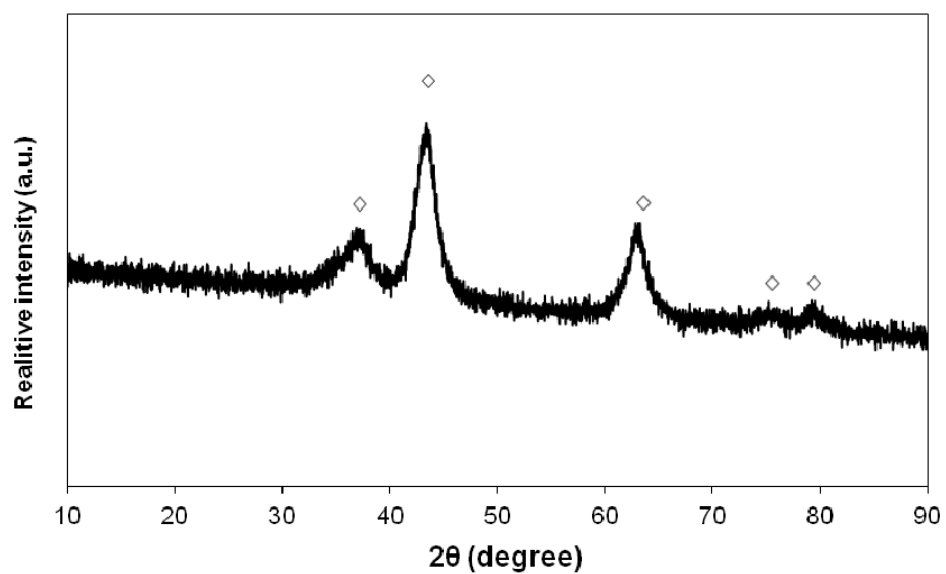**Fig. 9.** XRD pattern of calcined 30%Ni-10%Co hydrotalcite catalyst. Peaks marked with (◇) are characteristic of NiO, MgO, $MgNiO_2$, Co_3O_4, $CoAl_2O_4$, $NiAl_2O_4$, $MgCo_2O_4$ and Al_2MgO_4.

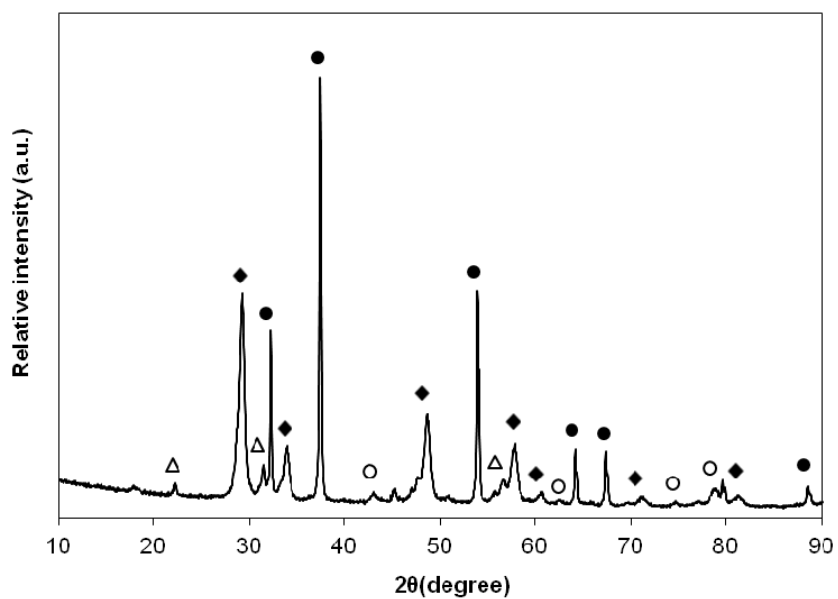**Fig. 10.** XRD pattern of CaCeZr (10:1:1) and 30%Ni-10%Co hydrotalcite catalyst after seven cycles of SEWGS. CaO (●), $Ce_{0.5}Zr_{0.5}O_2$ (◆) $CaZrO_3$ (△) NiO (○).